Molecular Cell, Vol. 20, 951–962, December 22, 2005, Copyright ©2005 by Elsevier Inc. DOI 10.1016/j.molcel.2005.10.030

The Role of Docking Interactions in Mediating Signaling Input, Output, and Discrimination in the Yeast MAPK Network

Attila Reményi,[1] Matthew C. Good,[1,2] Roby P. Bhattacharyya,[1,2] and Wendell A. Lim[1,2,*]
[1] Department of Cellular and Molecular Pharmacology
[2] Program in Biological Sciences
University of California, San Francisco
600 16th Street
San Francisco, California 94143

Summary

Cells use a network of mitogen-activated protein kinases (MAPKs) to coordinate responses to diverse extracellular signals. Here, we examine the role of docking interactions in determining connectivity of the yeast MAPKs Fus3 and Kss1. These closely related kinases are activated by the common upstream MAPK kinase Ste7 yet generate distinct output responses, mating and filamentous growth, respectively. We find that docking interactions are necessary for communication with the kinases and that they can encode subtle differences in pathway-specific input and output. The cell cycle arrest mediator Far1, a mating-specific substrate, has a docking motif that selectively binds Fus3. In contrast, the shared partner Ste7 has a promiscuous motif that binds both Fus3 and Kss1. Structural analysis reveals that Fus3 interacts with specific and promiscuous peptides in conformationally distinct modes. Induced fit recognition may allow docking peptides to achieve discrimination by exploiting subtle differences in kinase flexibility.

Introduction

MAPKs are central nodes in a complex signal transduction network that allow eukaryotic cells to respond to a broad set of environmental signals. MAPKs must interface with a diverse set of partners—upstream activating kinases, deactivating phosphatases, and substrates. Moreover, because cells contain multiple MAPK pathways, these interactions must be discriminatory so that the proper response is elicited by a specific stimulus. MAPK network wiring is further complicated by the fact that in some cases a subset of the same protein components is used within distinct MAPK pathways. In these cases, MAPK interactions must be promiscuous. How is this balance between specificity and promiscuity maintained?

It has been proposed that MAPK docking motifs may form a modular recognition system mediating connectivity (Fantz et al., 2001; Jacobs et al., 1999; Tanoue et al., 2000; Vinciguerra et al., 2004). Docking motifs are short peptide sequences, often found in substrates, that bind to a groove on the MAPK surface distinct from the kinase active site. The presence of docking motifs in substrates contributes to the efficiency with which they are phosphorylated (Sharrocks et al., 2000; Barsyte-Lovejoy et al., 2002). Growing evidence indicates that docking interactions also mediate interactions with upstream factors; putative docking motifs are found in other components of MAPK pathways, including activators, phosphatases, and scaffold proteins (Biondi and Nebreda, 2003; Tanoue and Nishida, 2003).

Saccharomyces cerevisiae has at least four distinct MAPK pathways involved in mating, filamentous growth, osmolarity response, and cell wall integrity. In the mating pathway, response to the pheromone α factor is mediated by the MAPK Fus3. Proteins known to physically interact with Fus3 include the upstream activating kinase Ste7 (Errede et al., 1993), the inactivating phosphatase, Msg5 (Doi et al., 1994), and the scaffold Ste5 (Choi et al., 1994), as well as substrates such as Far1 (Peter et al., 1993). These proteins contain sequences that match the general MAPK docking motif $(R/K)_{1-2}X_{4-6}LXL$. Connectivity within yeast MAPK networks is complicated by the fact that functionally distinct pathways use overlapping sets of protein components (Madhani and Fink, 1998; Breitkreutz and Tyers, 2002). For example, the MAPKK Ste7 participates in both the mating and filamentation pathways (starvation induced filamentous growth; [Cook et al., 1997]): it is the upstream activator of two MAPKs, Fus3 (mating) and Kss1 (filamentation). Despite high similarity, these two MAPKs yield distinct phenotypic output responses. The overlapping yet distinct subsets of functional interactions of particular MAPKs raises the question of whether docking motifs contribute to specificity by discriminating between MAPKs or if they are relatively promiscuous in their interactions with the various members of the MAPK family.

Here, we demonstrate that MAPK docking motifs are critical elements in directing kinase-specific signal flow within the overall yeast MAPK network; they are essential for efficient signaling both to and from the MAPK. Although Fus3 and Kss1 bind with similar affinity to many of their docking partners, including their common upstream activator, the MAPKK Ste7, we find that docking motifs from certain partners, such as the mating-specific cell cycle regulator protein Far1, are discriminatory, binding selectively to Fus3. We have solved the crystal structures of Fus3 alone and in complex with both promiscuous and selective docking peptides and find that these two classes of ligands bind in distinct conformational modes. Induced fit interactions may allow docking motifs to probe differences in docking site flexibility to achieve discrimination between highly homologous kinases.

Results and Discussion

Affinity and Specificity of Docking Motifs from Diverse MAPK Interacting Proteins

Putative docking motifs have been reported in diverse proteins functionally linked with the mating MAPK Fus3. These include upstream positive (e.g., MAPKK Ste7) and negative regulators (e.g., phosphatase Msg5), and downstream substrates (e.g., Far1) (Figure 1A). Our goal was to identify bona fide motifs from these proteins that directly bound to Fus3 in vitro. To address issues of

*Correspondence: lim@cmp.ucsf.edu

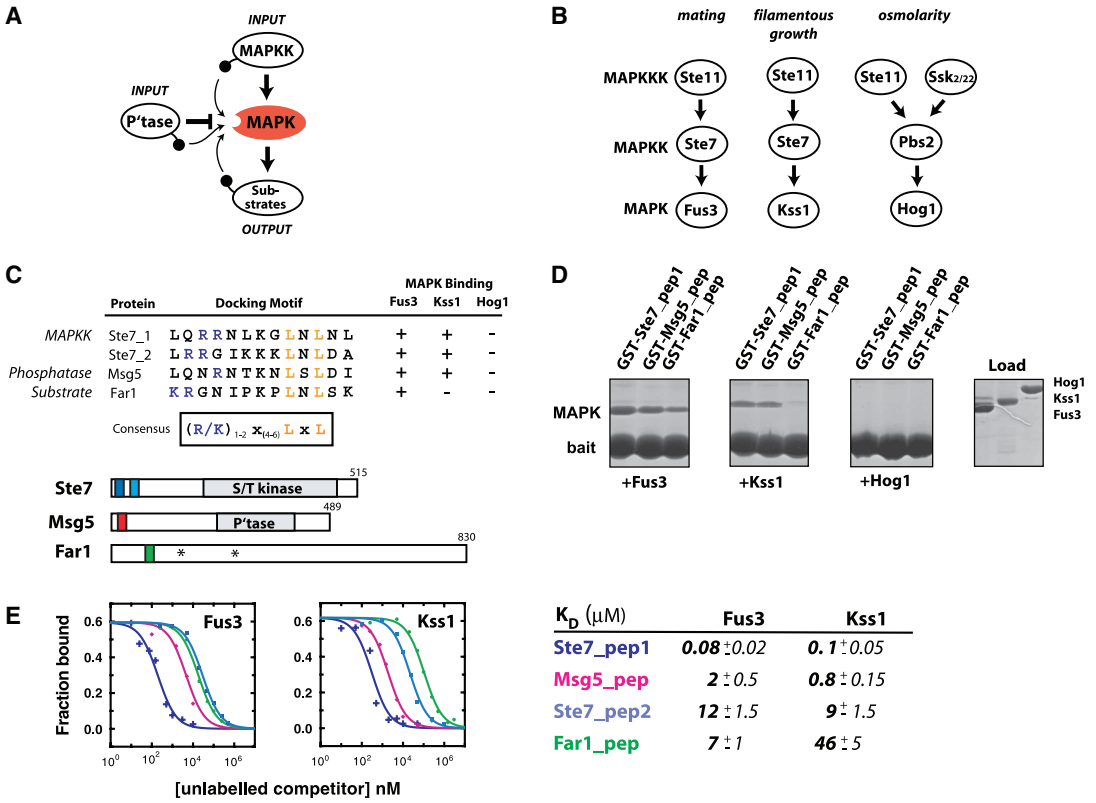

Figure 1. Docking Motifs Found in Interaction Partners of the *Saccharomyces cerevisiae* MAPKs Fus3 and Kss1

(A) MAPK activity is regulated by an upstream MAPKK (activating) and phosphatases (inactivating). The MAPK itself regulates the activity of downstream substrates. All three classes of partners contain putative docking motifs.

(B) Three distinct MAPK pathways in *Saccharomyces cerevisiae* utilize three different MAPKs (Fus3, Kss1, and Hog1), but their upstream activation involves shared kinase components (e.g., Ste11 and Ste7).

(C) Docking motifs found in various MAPK interacting partners. Their position in the full-length proteins are shown below. Summary of binding interactions (see [D]) is given.

(D) Testing MAPK interaction specificities of putative docking motifs. Purified MAPKs were used in pull-down binding assays with GST-docking motif fusion proteins. Bound kinases were detected by Coomassie staining.

(E) Quantitative binding of docking peptides to Fus3 and Kss1 measured by competition fluorescence polarization binding assays. Error bars indicate uncertainty of the fit to a competition binding equation.

specificity, we tested motifs for binding to other yeast MAPKs, including the closely related filamentation MAPK Kss1 and the more distantly related osmolarity MAPK Hog1 (Figure 1B).

Sequence analysis of Ste7, Msg5, and Far1 reveals one or more putative docking consensus motifs (Figure 1C). Putative motifs were cloned as GST fusions and screened for binding to purified Fus3, Kss1, and Hog1 (Figure 1D). We identified two such motifs in Ste7, including one that had previously been reported (Bardwell et al., 1996) (here referred to as Ste7_pep1) and one that is reported in this study (Ste7_pep2). We probed the specificity of these docking motifs for other yeast MAPKs such as Kss1 and Hog1. Hog1 did not bind to any of the Fus3 binding motifs. Kss1 bound tightly to the motifs from Ste7 and Msg5, but not to the motif from Far1. The differential binding of these two MAPKs to the docking motif of Far1 is particularly interesting because Far1 is a pivotal component of mating-stimulated cell cycle arrest and is phosphorylated preferentially by Fus3 (Breitkreutz et al., 2001). Far1 phosphorylation is relatively unaffected by loss of Kss1. Thus, the unique preference of the Far1 docking motif for Fus3 may play an important role in determining kinase-specific pathway outputs.

We used a fluorescence-based binding assay to quantitate docking affinities (Figure 1E). Docking peptides from Ste7 and Msg5 bind with similar affinities to both Fus3 and Kss1. In contrast, the Far1 peptide displayed a 7-fold preference for Fus3 over Kss1. The Fus3 binding motifs examined here all clearly discriminate between Fus3 and the distantly related MAPK Hog1; only a subset, however, discriminate between Fus3 and the closely related MAPK Kss1. Thus, docking motifs appear capable of displaying both high- and low-resolution specificity, and this specificity may be an important factor in wiring complex signal transduction pathways.

Docking Interactions Are Required for MAPK Activation by MAPKK Ste7

To examine the role of docking in MAPK activation by an upstream MAPKK, we expressed and purified a constitutively active version of the MAPKK Ste7 containing phosphomimicking mutations in its activation loop (S359E, T363E—referred to as Ste7EE) (Maleri et al.,

2004). Ste7EE can phosphorylate Kss1 in vitro. We chose to focus on the mechanism of Ste7EE activation of Kss1, rather than Fus3, because Ste7EE cannot phosphorylate Fus3 in a purified system (Fus3 activation also requires the scaffold protein Ste5; [Flatauer et al., 2005; A.R., unpublished data]).

Mutation of either or both of the Ste7 docking motifs does not affect the catalytic function of Ste7EE, as assayed by its ability to phosphorylate the model substrate myelin basic protein (MBP) (Figure S1 available in the Supplemental Data with this article online). These docking sites, however, are essential for Ste7EE to phosphorylate Kss1 (Figures 2A and 2B). Although mutation of either individual motif has little effect, simultaneous mutation of both motifs disrupts Kss1 phosphorylation. Thus, the two docking motifs are redundant but essential. We further examined the importance of the Ste7 docking motifs for Kss1 activation in vivo (Figure 2C). Although the physiological input for activation of the filamentation pathway (Ste11 → Ste7 → Kss1) is starvation, addition of α factor leads to low but detectable expression of a filamentation reporter gene (*f*ilamentation and invasion growth *r*esponsive *e*lement [FRE] fused to *lacZ*) (Madhani and Fink, 1997). Mutation of the individual Ste7 docking motifs leads to a mild loss of FRE gene expression in a ΔSte7 strain (MG40; see Table S1). In agreement with the in vitro analysis, however, loss of both docking motifs abolishes FRE expression, demonstrating that docking interactions are critical for MAPKK → MAPK information flow.

Role of Docking Interactions in MAPK Inactivation by the Phosphatase Msg5

MAPKs are also regulated by phosphatase-mediated inactivation. We have identified one strong docking motif in the phosphatase Msg5, a protein previously shown to downregulate Fus3 (Andersson et al., 2004; Zhan et al., 1997). However, by sequence analysis, several potential weak docking motifs can be found. Thus, to eliminate potentially redundant docking interactions (as in the case of Ste7), we used a version of Fus3 bearing a mutation (Asp314 → Lys and Asp317 → Lys; referred to as Fus3DDKK) previously shown to disrupt the docking groove of many MAPKs (Kusari et al., 2004). This mutation eliminates binding between Fus3 and the docking motifs in a GST-pull-down assay without altering catalytic activity toward the model substrate MBP (Figure S2). Thus, the Fus3 DDKK mutant provides a simple way to probe importance of docking interactions.

Disruption of docking interactions severely impairs desphosphorylation of Fus3 by Msg5 (Figures 2D and 2E). The effects are specific to Msg5, because Fus3 wild-type (wt) and Fus3 DDKK are equally good substrates for the nondocking-dependent λ-phosphatase. Thus, the docking interaction dramatically increases the ability of Msg5 to inactivate its cognate MAPK. To determine the importance of docking interactions for phosphatase-mediated regulation in vivo, we tested the effect of docking mutations on expression of the mating reporter gene Fus1-*lacZ* (Figure 2F). Msg5 has been shown to limit the level of Fus3 activation both in uninduced and α factor-stimulated cells: ΔMsg5 cells show elevated mating pathway transcription. We transformed ΔMsg5 strain (MG20) with either wt or docking-deficient Msg5 (primary docking motif containing four alanine substitutions: Msg5ND). Wt Msg5 decreases mating pathway output significantly compared to vector alone. However, Msg5ND only partially decreases mating output levels. This partial phenotype could be attributed to the presence of redundant Fus3 docking motifs in Msg5. Nonetheless, these data are consistent with docking interactions contributing to the ability of Msg5 to control Fus3 activity.

Docking Interactions Are Required for Far1-Mediated Cell Cycle Arrest during Mating

The output of MAPK pathways is determined by the specific substrates that each MAPK acts upon. The Fus3 substrate Far1 contains a docking motif that has the unusual property of discriminating between Fus3 and the closely related kinase Kss1 (54% identity; 71% similarity, Figure S3). Far1 phosphorylation is required for cell cycle arrest during mating, and this response is dependent on Fus3 (Figure 2G) (Breitkreutz et al., 2001). We hypothesized that docking interactions might play a critical role in encoding this pathway specific output.

We therefore tested if the Far1 docking interaction was required for its phosphorylation by Fus3 and for Far1-mediated cell cycle arrest. As an in vitro substrate, we used a minimal version of Far1 (mini-Far1, residues 1–393) that is fully functional for cell cycle arrest in vivo. Mini-Far1 contains two SP or TP motifs (Ser87 and Thr306) that are phosphorylated by Fus3 in response to α factor (Gartner et al., 1998). Wt Fus3 can potently phosphorylate mini-Far1 in vitro; however, a docking-deficient mutant of Fus3 (Fus3 DDKK) cannot (Figure 2H). In a converse experiment, we found that mutation of the Far1 docking motif (mini-Far1ND) also blocks phosphorylation by Fus3. Thus, the docking interaction is critical for efficient phosphorylation of Far1 by Fus3. In contrast, purified Kss1, which can phosphorylate the model substrate MBP, is unable to efficiently phosphorylate mini-Far1 or mini-Far1ND. The inability of Kss1 to recognize the Far1 docking motif makes this cell cycle arrest protein a highly specific substrate.

In parallel, we tested the importance of the Far1 docking motif for proper mating signaling in vivo, using cell budding and halo assays to monitor α factor-induced cell cycle arrest (Figure 2I). Upon α factor treatment, a type cells stop budding as they arrest in the G1 stage of the cell cycle. Deletion of Far1 (strain CB009) blocks mating-induced arrest: no halo (an area of low growth) is formed around discs of α factor, and cultures treated with α factor also display a high ratio (2/3) of budded (nonarrested) cells. Wt Far1 rescues this defect, yielding a strong arrest response. We find, however, that a version of Far1 in which the docking motif is mutated (Far1ND) fails to rescue this defect.

Crystal Structure of Fus3 MAPK

To date, none of the yeast MAPKs has been structurally characterized. We obtained crystals of the nonphosphorylated state of Fus3, as well as a nonphosphorylatable mutant in which the activation loop residues Thr180 and Tyr182 were mutated to Val and Phe, respectively (Fus3VF) (Table 1). The protein sequences of known MAPKs are well conserved from yeast to human (Fus3 is 51%, 44%, and 39% identical to ERK2,

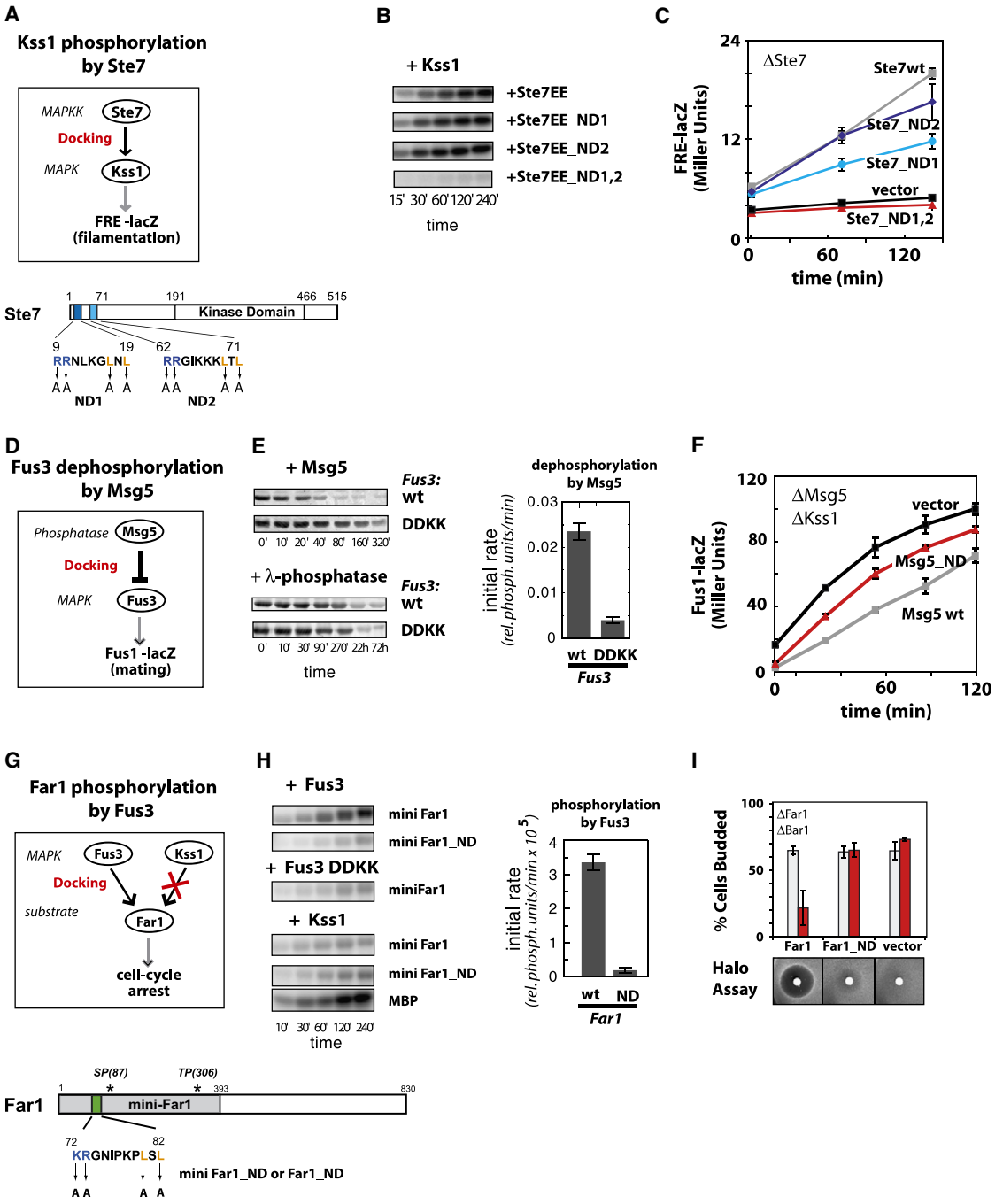

Figure 2. Docking Motifs Are Necessary for MAPK Phosphorylation by Ste7, Dephosphorylation by Msg5, and MAPK-Specific Phosphorylation of Far1

(A) The MAPKK Ste7 activates the MAPK Kss1 as part of the filamentation pathway. Ste7 has two MAPK docking motifs at its N terminus, which can be disrupted by mutating key interacting residues to alanines (mutations ND1 and ND2).

(B) In vitro Kss1 phosphorylation assays using purified constitutively active mutant of Ste7 (Ste7EE) bearing docking motif mutations. Phosphorylation is monitored by incorporation of radioactive phosphate. Disruption of both motifs eliminates Kss1 phosphorylation.

(C) In vivo induction of a Kss1-dependent filamentation reporter gene (FRE-*lacZ*) upon α factor stimulation is blocked when Ste7-Kss1 docking is disrupted in strain MG40 (red line). Docking motifs on Ste7 appear to be redundant.

(D) The phosphatase Msg5 downregulates activity of the mating MAPK Fus3.

(E) In vitro assay of Fus3 dephosphorylation by Msg5. Prephosphorylated Fus3 is treated with phosphatase, and loss of phosphorylation is monitored by using a phosphoprotein stain. Mutation in the docking groove of Fus3 (D314K, D317K—referred to as DDKK mutant) impairs dephosphorylation by Msg5 but has no effect on dephosphorylation by λ-phosphatase.

(F) In vivo assay of Msg5 function. In the absence of Msg5 (strain MG20), an elevated level of mating reporter gene (Fus1-*lacZ*) expression is observed upon stimulation with α factor (black line). Wild-type Msg5 (gray line) rescues this defect (lowering Fus1-*lacZ* expression). Msg5_ND is only able to partially restore lower expression.

(G) The cell cycle arrest factor Far1 is phosphorylated only by the MAPK Fus3 and not by Kss1. Far1 contains a single docking site shown below. Sites of phosphorylation as well as minimal functional Far1 (mini-Far1) are indicated.

Table 1. Crystallographic Data and Refinement Statistics

	Fus3 Nonphosph	Fus3VF	Fus3VF– Ste7_pep1	Fus3VF– Msg5_pep	Fus3VF– Far1_pep
Space group	$P2_12_12_1$	$P2_12_12_1$	$P2_12_12_1$	$P2_12_12_1$	$P2_12_12_1$
Resolution range (Å)	50–1.8	50–1.55	50–1.55	50–2.5	50–2.3
Number of data	28,329	43,406	52,829	13,279	16,794
Completeness (%)	96.4	94.9	96.9	98.1	97.5
Multiplicity	3.0	3.7	2.5	3.4	3.4
R_{sym}[a,b]	7.6 (14.0)	6.3 (26.6)	3.5 (23.2)	4.8 (12.5)	9.0 (31.2)
$I/\sigma I$[a]	9.0 (5.8)	14.4 (2.9)	26.6 (3.8)	18.7 (6.9)	12.4 (4.0)
R_{cryst}[c]	21.3	19.3	18.7	20.2	19.6
R_{free}[c]	25.9	23.1	21.6	27.9	26.3
Number of atoms	3010	3085	3230	2955	3095
<B> protein (Å^2)	22	20	17	29	25
<B> peptide (Å^2)	–	–	32	48	49
Rmsd bonds (Å)	0.010	0.015	0.014	0.013	0.011
Rmsd angle (º)	1.5	1.7	1.6	1.6	1.5

[a] Values in parentheses are for the highest resolution shell.
[b] $R_{sym} = \Sigma_{hkl}\Sigma_i |I_i(hkl) - \langle I(hkl)\rangle| / \Sigma_{hkl}\Sigma_i I_i(hkl)$.
[c] R_{cryst} and $R_{free} = |\Sigma F_{obs} - F_{calc}|/ \Sigma F_{obs}$; R_{free} is calculated with 10% of the data that were not used for refinement.

p38, and JNK3, respectively—Figure S3). The overall fold of Fus3 is highly homologous to that of mammalian MAPKs (Figure 3A). The crystal structure of Fus3VF is essentially identical to the nonphosphorylated form (npFus3, rmsd for 337 Cα positions is 0.46 Å). These structures likely represent the inactive state of Fus3. Loss of phosphorylatable residues in the activation loop renders Fus3VF incapable of mediating mating response in vivo (Gartner et al., 1992). Moreover, both Fus3VF and npFus3 show low activity in vitro. Fus3 can be phosphorylated in vitro, however, by extended incubation with ATP, which results in autophosphorylation. Once activated in this manner, Fus3 readily phosphorylates MBP (Figure S4).

Protein kinases are molecular switches that adopt "on" and "off" states. Some kinases are regulated through allosteric shifts in the position of catalytic residues. Alternatively, other kinases are regulated through a pseudo-substrate mechanism in which an inhibitory segment or binding partner occludes substrate binding (Huse and Kuriyan, 2002). The inactive Fus3 structure is consistent with a pseudo-substrate mechanism of regulation; key catalytic residues of inactive Fus3 appear to be already positioned in an active configuration (Figure 3B). However, substrate access to the active site appears to be blocked by residues 180–186, which contain or directly follow the phosphorylatable Thr180 and Tyr182 residues in the activation loop. The position at which these residues interact is similar to that occupied by peptide inhibitors of PKA (Figure 3C) (Knighton et al., 1991).

Structure of Fus3 Complexed with Promiscuous Docking Motifs from Ste7 and Msg5

We determined the crystal structure of Fus3VF in complex with docking peptides from Ste7 and Msg5 (high affinity site, Ste7_1: RRNLKGLNLNLHPD; Msg5, PRSLQNRNTKNLSLDIAALHP—visible regions underlined; Figure 4A and Figure S5). No long range structural changes in the kinase fold or kinase active site residues are induced upon docking motif binding, consistent with the observation that these peptides do not significantly alter catalytic activity (data not shown). Both docking motifs bind to the same surface on the opposite side from the Fus3 active site, the same site as for the mammalian MAPKs p38 and JNK1 (Chang et al., 2002; Heo et al., 2004).

There are two major elements found in nearly all MAPK docking motifs: a cluster of basic residues at the N terminus and a hydrophobic motif near the C terminus. These elements are recognized by complementary surfaces on the kinase surface (Figure 4B). The basic motifs bind to a negatively charged surface on Fus3 formed by the side chains of Glu69, Asp314, and Asp317 (earlier described as the common docking or CD site; [Tanoue et al., 2000]). The salt-bridge interactions made by these Asp residues explain why their mutation (Fus3DDKK mutant described previously) disrupts docking. The hydrophobic motif binds to a series of shallow hydrophobic pockets on the kinase surface. These pockets are defined by the kinase's hinge region and the loops between β8-β9 and α2-α3. This region of the kinase was previously named the ϕxϕ groove (Chang et al., 2002). However, by comparing the current and previous structures, we now know that there are actually three (not two) hydrophobic pockets on this surface, which we will call A, B, and C, that bind the motif LxLxL/I found in both the Ste7 and Msg5 peptides. Deletion studies (data not shown) suggest that the most C-terminal hydrophobic residue in the LxLxL/I motif is the least critical for Fus3 binding.

(H) In vitro analysis of Far1 phosphorylation by Fus3 and Kss1 mutants, measured by ^{32}P incorporation into Far1. Mutation of the docking motif in mini-Far1 disrupts its ability to serve as a substrate for Fus3. Conversely, mutation of the Fus3 docking site (DDKK) disrupts its ability to phosphorylate mini-Far1. Kss1 does not effectively phosphorylate mini-Far1, either with or without a docking motif, though it can phosphorylate MBP.
(I) In vivo analysis of cell cycle arrest mediated by full-length Far1 variants in strain CB009. Arrest was detected by counting budded cells (top: gray bars, untreated; red bars, α factor treated) or by halo assays (bottom). Far1 containing a docking site mutation (Far1_ND) cannot mediate arrest.
In (E) and (H), error bars indicate uncertainty in the fit to a first order polynomial equation at the linear part of the curves. In (C), (F), and (I), error bars represent standard deviation from three independent experiments.

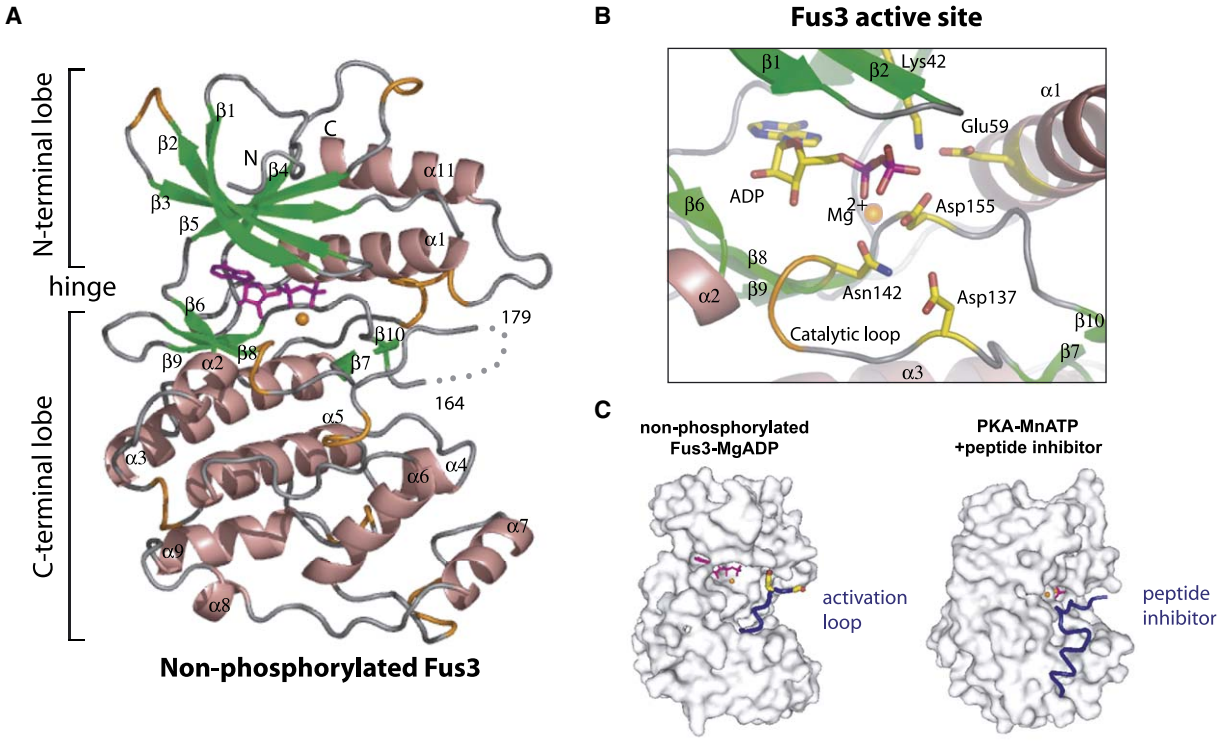

Figure 3. Structure of the Fus3 MAPK

(A) Overall structure of nonphosphorylated Fus3.

(B) Close-up view of Fus3 active site. The key catalytic residues appear to be in functional position.

(C) Comparison of inactive Fus3 structure with structure of PKA catalytic subunit in complex with a 20 residue peptide inhibitor (Knighton et al., 1991). Part of the activation loop of Fus3 appears to occlude substrate access, much as the PKA inhibitor does.

Comparison of these structures with mammalian docking structures (Figure 4C and Figure S6) suggests that spacing between the basic and hydrophobic elements is important for recognition. In the case of the Ste7 and Msg5 docking peptides, there are four intervening residues between the basic cluster and the LxLxL/I element. These residues are well conserved between the two peptides and form an identical β turn. This turn is stabilized by three intramolecular hydrogen bonds: one between the backbone atoms of residues i and i + 3 and two between a conserved Asn side chain and the peptide main chain (Figure 5A). In the p38 and JNK complexes, no such tight β turn is observed in the docking peptide intervening region. However, in these peptides, the intervening region is shorter—it is less than three residues long. Thus, the β turn observed in the Ste7 and Msg5 peptides appears to be an energetically favorable way for the peptide to effectively shorten its longer intervening region, allowing the peptide to maintain proper spacing between the basic and hydrophobic clusters. The alternative ways in which intervening regions can span the proper distance between the two key interaction points may explain why there is high apparent variability in the length of this region.

Docking Discrimination: Far1 Motif Binds Fus3 in a Conformationally Distinct Mode

We were also able to solve the crystal structure of Fus3 in complex with the discriminatory docking peptide from Far1. Although the Far1 peptide binds at the same site, it adopts a very different conformation from the other ligands. This interaction represents an alternative mode of binding, which we refer to as mode 2. This new mode of binding requires some rearrangement of the Fus3 surface: the shape of the hydrophobic binding pockets and the network of hydrogen bonding residues that interact with the peptide main chain both subtly shift (Figure 5B).

In the Ste7 and Msg5 complexes (mode 1), the hydrophobic pockets A, B, and C interact with the underlined side chains within the docking motif LxLxL/I. In contrast, in the Far1 complex (mode 2), the peptide residues that dock in these pockets have a different spacing: PKPLNL (Figure 5A). The A like pocket in mode 2 is slightly smaller and is further from the B pocket, and we refer to this altered pocket as the A′ site. The shifts observed in the mode 2 complex allow accommodation of two intervening residues between the A′ and B binding side chains as well as increased steric complementarity to the Pro residue that now inserts in the A′ site. As part of this shift, the kinase side chains Asp112 and Tyr312 move to form a different set of hydrogen bonds with the peptide main chain (Figure 5B). The use of Tyr312 as part of the A′ pocket to recognize the peptide proline is reminiscent of the mechanism used by many proline recognition domains: a Tyr is often used because its planar structure allows parallel packing against the nearly planar Pro side chain, while its hydroxyl group is then well positioned to interact with the main chain (Zarrinpar et al., 2003a).

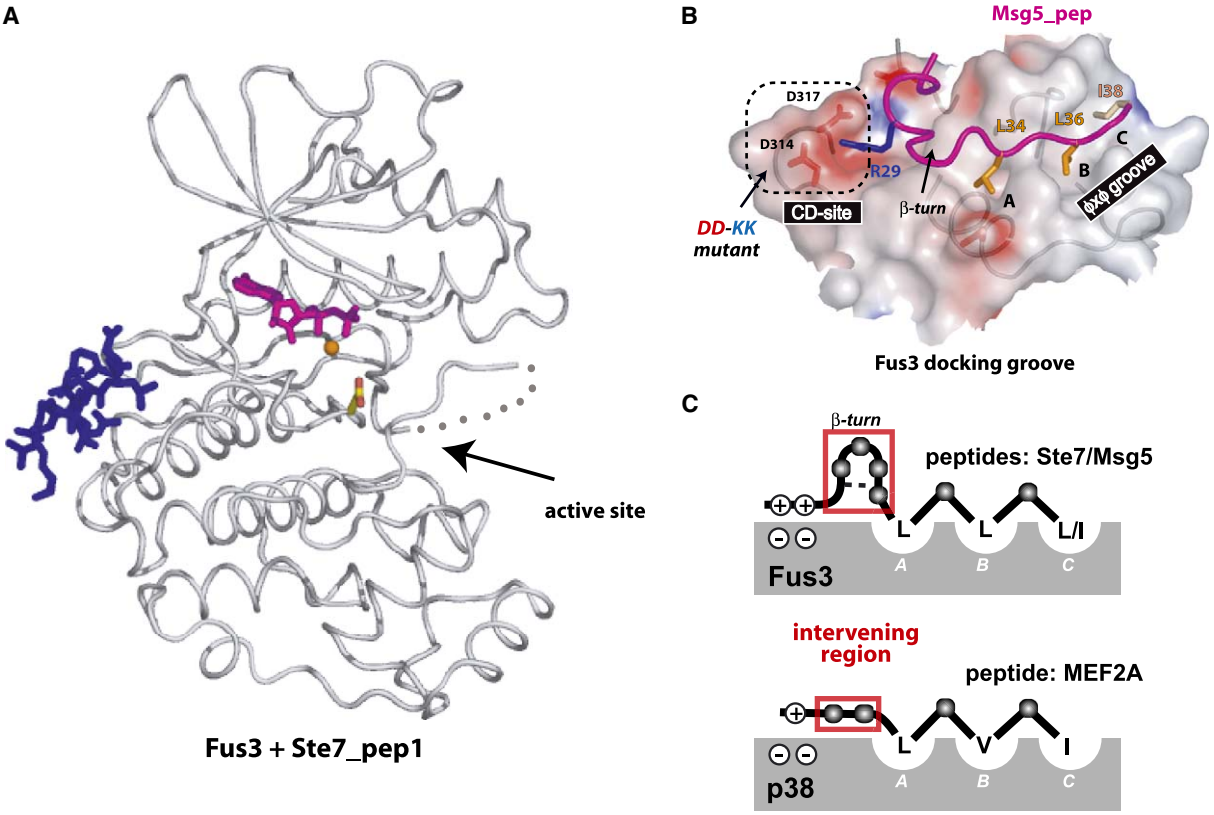

Figure 4. Structure of Fus3 in Complex with Promiscuous Docking Motifs from Ste7 and Msg5

(A) Overall structure of Fus3/Ste7 docking complex. Ste7 peptide is shown in purple and ATP in magenta.

(B) Close up of Fus3/Msg5 docking surface shows two main regions of interaction: the hydrophobic groove, which has three side chain docking pockets (A, B, and C; B and C were earlier described as "ϕ-x-ϕ groove"), and the acidic region, known as the "common docking" (CD) site, which binds the basic residues at the N terminus of the docking motifs. The DDKK mutation involves charge reversal of CD site residues.

(C) Cartoon of MAPK docking surface comparing Fus3-Ste7 complex with the mammalian p38-MEF2A complex. Both peptides display similar interactions with the two main regions of the MAPK but have different conformations in the intervening region between the basic and hydrophobic motifs.

There are at least two potential reasons why the Far1 peptide is incompatible with mode 1 interaction (Figures 5C and 5D). First, if the same spacing was maintained, the side chains KxLxL would insert into the hydrophobic pockets, resulting in burial of the hydrophilic Lys side chain. Second, Pro77 from the Far1 peptide would be in a position that, based on phi-psi restrictions, forbids proline (first position in the β turn). The two Pro residues in Far1 are thus much more likely to favor the polyproline II conformation that is observed in mode 2 binding. Although interaction of Far1 in this new mode is considerably weaker than that of Ste7 (affinity for Fus3 is 100-fold reduced), it is still able to achieve tolerable complementarity, given the compensating reorganization that occurs on the Fus3 docking surface. Interestingly, the interaction of the docking peptide from Jip1 with the mammalian MAPK JNK1 also appears to occur via a mechanism similar to mode 2 (Figure S6).

Model for Docking Discrimination: Differential Flexibility of the Docking Groove

Why does the Far1 motif discriminate against Kss1? Far1 cannot bind to a MAPK docking groove through mode 1—the mode observed with the Ste7 and Msg5 ligands—for the reasons highlighted above. Fus3, however, can adjust through subtle induced fit conformational changes to interact with the Far1 motif in an alternative mode. Fus3 has sufficient flexibility to participate in two distinct modes of binding. Thus, a simple model for specificity is that Kss1 is unable to make the adjustments to participate in mode 2 binding, thus preventing recognition of Far1 (Figure 5E). Far1 and other peptides that are only compatible with mode 2 binding would be recognized selectively by Fus3. However, those peptides compatible with mode 1 binding would be recognized by both Fus3 and Kss1. It is possible that there are alternate modes of binding that would lead to Kss1 selective docking motifs. This appears to be an example of negative selection (against Kss1 binding) playing a major role in determining interaction specificity (Zarrinpar et al., 2003b).

Residues in Fus3 and Kss1 that directly contact the peptides are almost all identical. There are, however, several sequence differences in Kss1 that occur near the docking groove (Figure 5B). First, the linker between helices 2 and 3, both of which contain residues that hydrogen bond to the docking peptide backbone, has a five amino acid insertion in Kss1 relative to Fus3.

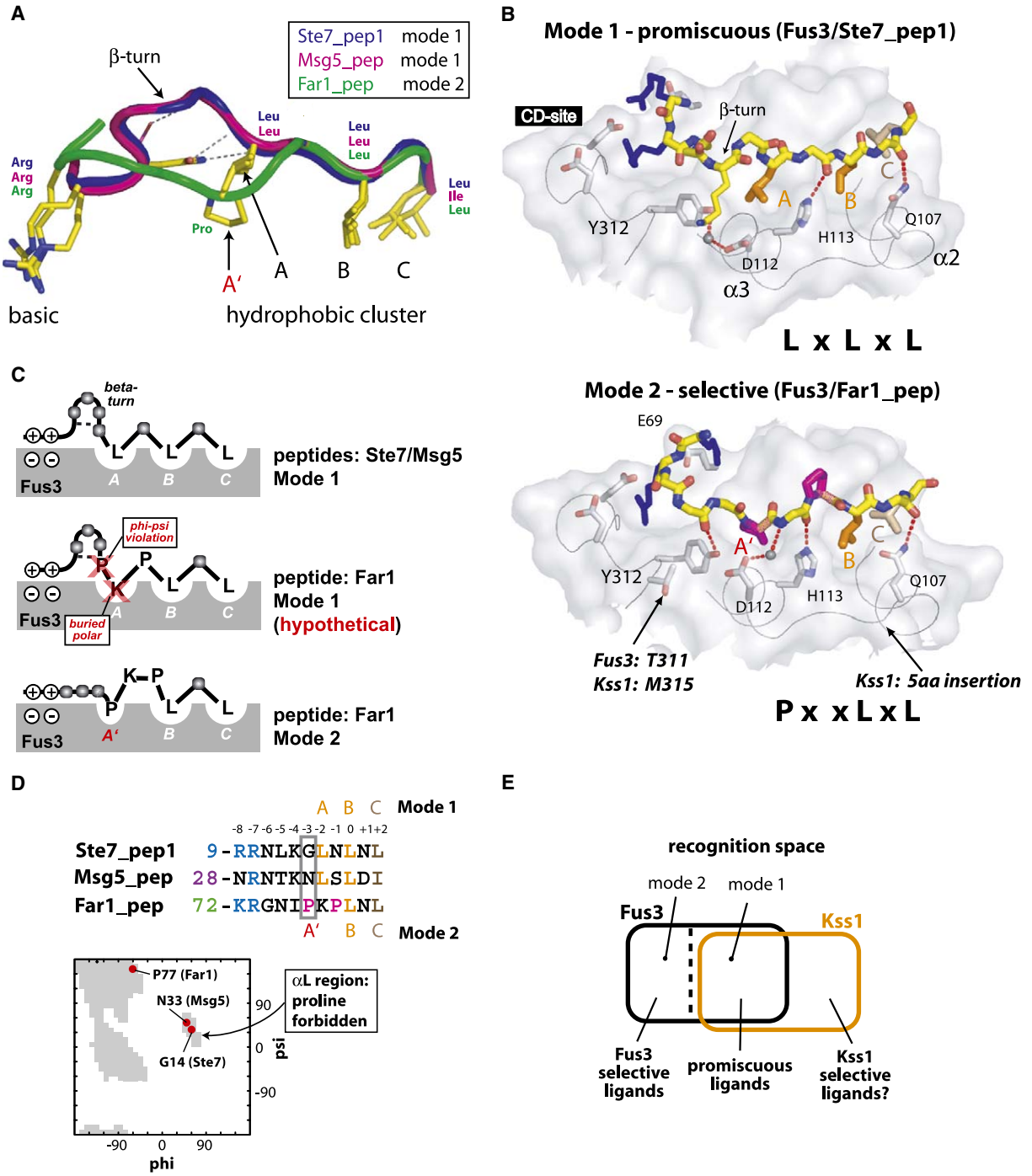

Figure 5. Structure of Fus3 in Complex with a Kinase Selective Docking Motif from Far1

(A) Far1 docking peptide (green) and Ste7 and Msg5 peptides (purple and magenta) bind in distinct modes. Peptide structures were aligned by using atoms from the N-terminal Arg and the C-terminal residues that pack into pockets B and C. Although all of the peptides achieve a similar overall spatial arrangement of the above anchor residues, the remaining regions show highly divergent conformations. The promiscuous peptides adopt an intervening β turn (mode 1), whereas the selective peptide lacks the turn and packs a different position into the A pocket (mode 2).

(B) Surface depictions of Fus3 in complex with promiscuous and selective peptides highlighting the different spacing of packing residues and the different pattern of main chain hydrogen bonding in the two modes of interaction. (For clarity, side chains atoms are shown only for selected residues.) In mode 2, the kinase surface adjusts the A pocket to achieve complementarity with Pro at this position and to make a new set of main chain hydrogen bonds. Regions of sequence divergence between Fus3 and Kss1 are labeled.

(C) Cartoon illustrating why Far1 peptide could not bind Fus3 in mode 1. Docking of Far1 peptide in mode 1 (middle) would lead to insertion of polar residue (Lys) in the A pocket and a Pro at a position at which proline is sterically forbidden (see [D]).

(D) Phi-psi plot of docking motif position P-3 (highlighted in gray box). Both G14(Ste7) and N33(Msg5) are at the end of the β turn and therefore fall in the left-handed α helix conformation (αL). This region of conformation space is forbidden to proline (i.e., for P77[Far1]). In mode 2, the two prolines in the Far1 peptide adopt the proline-preferred Polyproline II conformation.

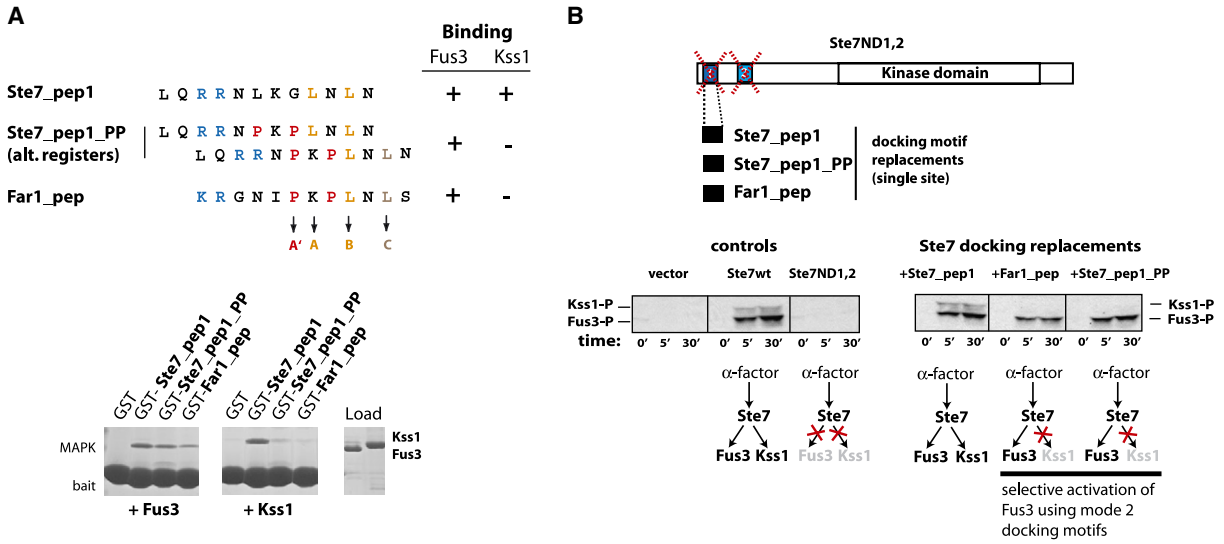

Figure 6. Signal Flow in MAPK Pathways In Vivo Can Be Redirected Based on Docking Motif Promiscuity/Selectivity

(A) Introduction of a PxP motif into Ste7_pep1 transforms a promiscuous docking motif into a selective one. The altered version of the Ste7 motif (Ste7_pep1_PP) is shown in two possible binding registers; Pro is introduced at the proline-forbidden position in either register. GST-pull-down assays demonstrating the selectivity of the mutant peptide are shown below.

(B) Replacement of promiscuous with discriminatory docking motifs in Ste7 can result in selective MAPK activation (phosphorylation). A Ste7 allele lacking both native docking sites was used as background; a single functional docking site that was either promiscuous (Ste7_pep1, wt) or selective (Far1 or Ste7_pep1_PP) was reintroduced. Phosphorylation of Fus3 and Kss1 upon α factor stimulation was detected by Western blot using a MAPK-activated state-specific antibody on yeast cell lysates (strain MG40). In the absence of Ste7 (vector), neither Kss1 nor Fus3 is activated (lanes 1–3). In the presence of Ste7wt, both MAPKs are readily phosphorylated (lanes 4–6). MAPK activation is abolished when both of the docking motifs are mutated (lanes 7–9). Reinsertion of the wild-type Ste7_pep1 docking motif restores efficient phosphorylation of both MAPKs (lanes 10–12). Replacement of the promiscuous site with a discriminatory docking motif such as Far1 (lanes 13–15) or Ste7_pep1_PP (lanes 16–18) specifically activates Fus3, but not Kss1.

Second, residue Thr311 in Fus3 is a Met (315) in Kss1. This residue packs immediately adjacent to Tyr312, which forms parts of pocket A′. It is possible that the larger Met side chain might alter the positioning or flexibility of the adjacent Tyr in Kss1. In addition, it is possible that many subtle differences between the Fus3 and Kss1 sequences are coupled to these fine-tuned differences in structure and flexibility.

Fus3-Specific Docking Motifs Are Sufficient to Direct Selective MAPK Activation by Ste7

To test the importance of discriminatory docking motifs in directing MAPK signaling, we explored whether promiscuous docking motifs could be made kinase selective. By our model, one reason the Far1 peptide cannot participate in mode 1 binding is because it has a proline at a position at which such a residue is sterically forbidden (the beginning of the intervening β turn). Thus, we introduced a proline into the equivalent position in the Ste7_1 peptide. Because of the three hydrophobic binding pockets and a possible binding register shift, both L12 and G14 in Ste7_pep1 were mutated to prolines. This peptide is referred to as Ste7_pep1_PP. Remarkably, these two mutations were sufficient to change Ste7_pep1 into a discriminatory peptide that could only bind Fus3 and not Kss1 in pull-down assays (Figure 6A).

Next, we tested whether discriminatory docking motifs could alter specificity of MAPK activation in vivo. Activated Ste7 phosphorylates both Fus3 and Kss1 because it has two promiscuous docking motifs (Ste7_pep1 and Ste7_pep2). We disrupted both native docking sites in Ste7 (Ste7_ND1,2) and replaced them with a single functional docking motif to test the ability of this motif to direct signal flow. Specificity of signaling was assayed by stimulating with α factor then monitoring the extent of Kss1 and Fus3 phosphorylation in Western blots by using an anti-phospho-MAPK antibody that recognizes both kinases (Figure 6B). When a functional Ste7_pep1 was reinserted into this background, phosphorylation of both Kss1 and Fus3 was observed, consistent with promiscuous interaction of Ste7 docking motifs with both MAPKs. However, if either the Far1 docking motif or the selective mutant Ste7_pep1_PP was inserted into this background, only activation of Fus3 was observed. These findings demonstrate that the docking motif sequence alone is sufficient to direct selective MAPK activation.

Conclusions: MAPK Docking Motifs as Organizational Tools for Complex Signal Transduction Pathways

Docking motifs play an important organizational role in mediating signal flow to and from yeast MAPKs. In

(E) Model for kinase selectivity. Fus3 has the conformational flexibility to recognize ligands in either mode 1 or 2. Kss1 can bind ligands in mode 1 but cannot adjust to bind mode 2 ligands, thus they are selective. It is possible that there are movements that Kss1 can undergo that allow it to selectively interact with a different class of ligands.

agreement with the central role of Ste7 in activation of both Fus3 and Kss1, the characterized docking motifs from Ste7 show nondiscriminatory interactions with the two related target kinases. In contrast, docking motifs can also modulate remarkably fine-tuned specificity: Far1 is a discriminating substrate that contains a docking motif that can uniquely bind Fus3 and not Kss1. A PxP motif, present within the Far1 docking sequence, is able to confer kinase selectivity upon a previously promiscuous docking sequence. Nondiscriminatory MAPK docking motifs are pivotal for signaling networks that use shared components and respond to similar upstream inputs. The existence of discriminatory docking motifs, on the other hand, is a great asset in correctly directing signal flow where required. Docking motifs appear to offer the flexibility of providing either low- or high-resolution specificity.

If docking interactions between MAPKs and their interaction partners are important for organizing signal flow, it is anticipated that these interactions and their different degrees of discrimination would be conserved in different organisms. Docking between MAPK/activator, MAPK/phosphatase, and MAPK/substrate pairs indeed appears to be a conserved trait among other fungal species (Figure S7). Moreover, the degree of kinase discrimination encoded in these interactions appears to be also conserved, because a PxP motif which is associated with high-resolution discrimination between Fus3 and Kss1 is found in all easily identifiable Far1 homologs.

MAPK docking sites are beginning to emerge as possible targets for drug design; because docking interactions are necessary for many MAPK connections, inhibition of the site can block function. For example, JNK docking inhibitors are showing promise as treatments for stroke, as they can inhibit ischemia-induced apoptosis, a JNK-mediated response (Borsello et al., 2003). Our findings that even very closely related docking sites have differences in steric and conformational properties that can be detected by peptide ligands bode well for the goal of generating docking site inhibitors that are highly kinase selective.

Experimental Procedures

Protein Expression and Purification

Fus3 was expressed in Rosetta(DE3)pLysS cells (Novagen) at 18ºC for 12 hr with N-terminal histidine tag. After affinity purification, the tag was removed by the TEV protease and the sample further purified by ion exchange (RESOURCE 15Q [Amersham]; 20 mM Tris [pH 8.0], 2 mM DTT, 10% glycerol, and 0–1 M NaCl). Recombinant Fus3 expressed in *E. coli* is partially phosphorylated (data not shown). Homogeneously nonphosphorylated protein (npFus3) was obtained by treatment with λ-phosphatase. In an alternative approach, we expressed a version of the protein in which the normally phosphorylated activation loop residues Thr180 and Tyr182 were mutated to valine and phenylalanine, respectively (Fus3VF).

Kss1, Hog1, Ste7EE (S359E, T363E), and the docking mutant versions thereof were expressed in SF9 insect cells, the two MAPKs with His tags, and the MAPKK as GST-fusion protein by using the Bac-to-Bac Baculovirus Expression System (Invitrogen). The test substrate protein MBP was purchased from Sigma (M1891). Mini-Far1 constructs (1–393 aa) and full-length Msg5 were expressed as fusion proteins with an N-terminal GST tag and a C-terminal 6×His tag in Rosetta(DE3)pLysS cells. Protein samples were first purified on Ni-NTA agarose then directly loaded to a GST column.

Peptides used for affinity measurements and crystallization were synthesized with standard Fmoc chemistry and purified by reverse-phase chromatography. Molecular masses were verified by mass spectrometry. GST-docking peptide fusion proteins were expressed in Rosetta(DE3)pLysS cells (Ste7_pep1, LQRRNLKGLNLN; Ste7_pep2, LRRGIKKKLTLD; Msg5_pep, PRSLQNRNTKNLSLD; Far1_pep, KRGNIPKPLNLS; and Ste7_pep1_PP, LQRRNPKPLNLN).

Crystallization and Data Collection

Crystallization trials were carried out at 20ºC by using hanging drops. Protein samples contained 20 mM Tris (pH 8.0), 100 mM NaCl, 10% glycerol, 2 mM TCEP, 2 mM $MgCl_2$, and 2 mM nucleotide cofactor (Fus3VF, ATP-γS or AMP-PNP; npFus3, ADP). The highest diffraction quality crystals grew from well solutions containing 25%–28% PEG1000, 0.1 M MES (pH 6.1), and 5%–10% MPD. Both crystals belonged to the same space group ($P2_12_12_1$) with identical cell dimensions (a = 57.3 Å, b = 62.5 Å, and c = 86.5 Å).

Fus3 complexes were formed by mixing Fus3VF protein with chemically synthesized peptides in a 1:2 molar ratio. The best crystals were obtained with a 14 mer (RRNLKGLNLNLHPD) for the Fus3/Ste7_pep1, with a 21 mer (PRSLQNRNTKNLSLDIAALHP) for the Fus3/Msg5_pep complex, and with a 13 mer (SKRGNIPKPLNLS) for the Fus3/Far1_pep complex. Binary protein-peptide complexes were grown in 15%–20% PEG 8000, 0.1 M MES (pH 6.1). All complex crystals belong to space group $P2_12_12_1$ with identical cell dimensions a = 58.3 Å, b = 63.8 Å, and c = 99.6 Å.

Single crystals were soaked in the appropriate well-solution supplemented with 25% (v/v) glycerol, mounted on nylon loops and flash-frozen in liquid nitrogen prior to data collection at 100 K. Datasets were collected at beamline 8.3.1 of the Advanced Light Source, Lawrence Berkeley National Laboratory. Data reduction and scaling was done with the HKL package (Otwinowski and Minor, 1997) (Table 1).

Structure Determination

The structure of Fus3 was solved by molecular replacement with the program AMoRe (Navaza, 1994) by using a poly-alanine version of ERK2 (Zhang et al., 1994) as a search model. The automated model building protocol of ARP 6.0 was used to refine and improve the initial model (Perrakis et al., 2001). ARP 6.0 could successfully build almost the entire model of Fus3. Additional model building was performed with O (Jones et al., 1991), and the structure was further refined with CNS (Brunger et al., 1998). The final model of Fus3 was then used as a search model in AMoRe to solve the structure of Fus3-peptide complexes.

The final models of npFus3, Fus3VF, Fus3/Ste7_pep1, Fus3/Msg5_pep, and Fus3/Far1_pep contain a full-length model of Fus3 (1–353) interspersed with a flexible segment encompassing part of the activation loop (164–179). This region appears to be flexible and invisible in all the structures. All crystal structures contain an ADP nucleotide in complex with one Mg^{2+} ion. Statistics are listed in Table 1.

In Vitro Experiments

Ste7_pep1 was synthesized with a cysteine at the C terminus and labeled with 5-iodoacetamide-fluorescein by a protocol suggested by the supplier (Molecular Probes). Change in peptide fluorescence polarization was monitored as a function of increasing concentration of purified Fus3 or Kss1 with an Analyst AD & HT Detection System (LJL Biosystems) plate reader in 384-well plates. The labeled peptide was present at 10 nM in 20 mM Tris-Cl (pH 8.0), 100 mM NaCl, 5 mM DTT, and 1 mg/ml BSA. The resulting binding isotherms were fit to a quadratic binding equation with ProFit 5.1.0 (Quantum Soft) as described elsewhere (Harris et al., 2001). The affinities of the labeled peptide for Fus3 and Kss1 were 50 nM and 120 nM, respectively. The affinities of the remaining, unlabeled peptides were measured by competition fluorescence polarization assays. Labeled Ste7_pep1 was at 10 nM, Fus3 or Kss1 were at 40 and 200 nM, respectively, and increasing amount of unlablelled peptide was added. The K_d for the unlabeled peptide was determined by fitting the data to a competition binding equation (Harris et al., 2001). In a typical GST-pull-down experiment, 10 μl of GST-resin saturated with bait was used and incubated in binding buffer (20 mM TrisCl [pH 8.0], 100 mM NaCl, 0.05% IGEPAL, and 2 mM TCEP) containing 10 μM prey.

To compare the activity of intact and mutated versions of Ste7EE on MAPK phosphorylation, Ste7 (~2 μM) was incubated with purified nonphosphorylated Kss1 (~8 μM) in kinase reaction buffer (20 mM Tris [pH 8.0], 150 mM NaCl, 0.05% IGEPAL, 2 mM TCEP, and 2 mM $MgCl_2$) containing 0.5 mM ATP and 5 μM radioactively labeled $ATP^{32}(\gamma)$. Core (nondocking-dependent) kinase activity was assessed by using MBP as a model substrate (concentrations of Ste7 and MBP were 10 and 50 μM, respectively.) In MAPK activity assays, purified enzyme (1 μM) was incubated with the different substrates (MBP, ~50 μM; mini-Far1, ~5 μM). Time course samples were run on SDS-PAGE, the gels dried, and radioactivity of the substrate bands were quantified by a phosphorimager screen and a Typhoon 8600 instrument. Initial phosphorylation rates were determined by fitting band signal intensity from the linear part of the time course.

For the in vitro phosphatase assays, preactivated Fus3 and Fus3DDKK were used as substrates. Five micromolars Fus3 or Fus3DDKK was incubated with 1.5 μM GST-λ-phosphatase or 0.25 μM GST-Msg5 protein. SDS-PAGE gels were stained with Pro-Q Diamond Phophoprotein Gel Stain (Molecular Probes). This fluorescent stain allows direct, in-gel detection of phosphate groups attached to tyrosine, serine, or threonine residues. Band intensities were scanned with a Typhoon 8600, and initial rates for dephosphorylation of Fus3 by Msg5 and lambda phosphatase were determined by fitting band signal intensity from the linear part of the time course to a first order polynomial equation.

In Vivo Experiments

Ste7, Msg5, or Far1 was expressed either from pRS314 (Trp1) or pRS316 (URA3) CEN/ARS plasmids (New England Biolabs). Plasmids contained the corresponding gene and its endogenous promoter. We used yeast strain (W303; *MATa his3 leu2 ura3 trp1*) as the parent strain for all knockouts. All experiments were performed in triplicate. β-galactosidase assays were used to monitor induction of Fus1-*lacZ* and FRE-*lacZ* as described previously (Sprague, 1991). Fus1-*lacZ* was integrated into the Mfa2 locus, and FRE-*lacZ* was maintained on a 2 μ plasmid. Halo assays were performed with the top-agar method as described earlier (Hoffman et al., 2002). Filter circles (1/4 inch) were spotted with 2.5 μg of α factor. Plates were grown at 30ºC for 36 hr and then scanned. Cell morphology was assayed by light microscopy to determine the percentage of budded cells after stimulation by α factor. Uninduced and α factor-induced (2 hr) cultures were fixed with 3.7% formaldehyde. Bud counting was done blinded. Western blots were carried out by using a MAPK-activation state-specific antibody that recognizes phosphorylated Fus3 as well as Kss1 (phospho-p44/p42 MAPK Thr202/Tyr204 antibody; Cell Signaling Technology).

Supplemental Data

Supplemental Data include seven figures and one table and can be found with this article online at http://www.molecule.org/cgi/content/full/20/6/951/DC1/.

Acknowledgments

This work was supported by a postdoctoral fellowship from the Jane Coffin Childs Memorial Fund (A.R.) and grants from the National Institutes of Health, Kirsch Foundation, and the Sandler Family Foundation (W.A.L.). We thank C. Bashor and other members of the Lim Lab for advice and assistance. We thank M. Schwartz and the Madhani Lab for the FRE reporter and other advice.

Received: May 17, 2005
Revised: September 7, 2005
Accepted: October 25, 2005
Published: December 21, 2005

References

Andersson, J., Simpson, D.M., Qi, M., Wang, Y., and Elion, E.A. (2004). Differential input by Ste5 scaffold and Msg5 phosphatase route a MAPK cascade to multiple outcomes. EMBO J. *23*, 2564–2576.

Bardwell, L., Cook, J.G., Chang, E.C., Cairns, B.R., and Thorner, J. (1996). Signaling in the yeast pheromone response pathway: specific and high-affinity interaction of the mitogen-activated protein (MAP) kinases Kss1 and Fus3 with the upstream MAP kinase kinase Ste7. Mol. Cell. Biol. *16*, 3637–3650.

Barsyte-Lovejoy, D., Galanis, A., and Sharrocks, A.D. (2002). Specificity determinants in MAPK signaling to transcription factors. J. Biol. Chem. *277*, 9896–9903.

Biondi, R.M., and Nebreda, A.R. (2003). Signalling specificity of Ser/Thr protein kinases through docking-site-mediated interactions. Biochem. J. *372*, 1–13.

Borsello, T., Clarke, P.G., Hirt, L., Vercelli, A., Repici, M., Schorderet, D.F., Bogousslavsky, J., and Bonny, C. (2003). A peptide inhibitor of c-Jun N-terminal kinase protects against excitotoxicity and cerebral ischemia. Nat. Med. *9*, 1180–1186. Published online August 24, 2003. 10.1038/nm911.

Breitkreutz, A., and Tyers, M. (2002). MAPK signaling specificity: it takes two to tango. Trends Cell Biol. *12*, 254–257.

Breitkreutz, A., Boucher, L., and Tyers, M. (2001). MAPK specificity in the yeast pheromone response independent of transcriptional activation. Curr. Biol. *11*, 1266–1271.

Brunger, A.T., Adams, P.D., Clore, G.M., DeLano, W.L., Gros, P., Grosse-Kunstleve, R.W., Jiang, J.S., Kuszewski, J., Nilges, M., Pannu, N.S., et al. (1998). Crystallography & NMR system: a new software suite for macromolecular structure determination. Acta Crystallogr. D Biol. Crystallogr. *54*, 905–921.

Chang, C.I., Xu, B.E., Akella, R., Cobb, M.H., and Goldsmith, E.J. (2002). Crystal structures of MAP kinase p38 complexed to the docking sites on its nuclear substrate MEF2A and activator MKK3b. Mol. Cell *9*, 1241–1249.

Choi, K.Y., Satterberg, B., Lyons, D.M., and Elion, E.A. (1994). Ste5 tethers multiple protein kinases in the MAP kinase cascade required for mating in S. cerevisiae. Cell *78*, 499–512.

Cook, J.G., Bardwell, L., and Thorner, J. (1997). Inhibitory and activating functions for MAPK Kss1 in the S. cerevisiae filamentous-growth signalling pathway. Nature *390*, 85–88.

Doi, K., Gartner, A., Ammerer, G., Errede, B., Shinkawa, H., Sugimoto, K., and Matsumoto, K. (1994). MSG5, a novel protein phosphatase promotes adaptation to pheromone response in S. cerevisiae. EMBO J. *13*, 61–70.

Errede, B., Gartner, A., Zhou, Z., Nasmyth, K., and Ammerer, G. (1993). MAP kinase-related FUS3 from S. cerevisiae is activated by STE7 in vitro. Nature *362*, 261–264.

Fantz, D.A., Jacobs, D., Glossip, D., and Kornfeld, K. (2001). Docking sites on substrate proteins direct extracellular signal-regulated kinase to phosphorylate specific residues. J. Biol. Chem. *276*, 27256–27265.

Flatauer, L.J., Zadeh, S.F., and Bardwell, L. (2005). Mitogen-activated protein kinases with distinct requirements for Ste5 scaffolding influence signaling specificity in Saccharomyces cerevisiae. Mol. Cell. Biol. *25*, 1793–1803.

Gartner, A., Nasmyth, K., and Ammerer, G. (1992). Signal transduction in Saccharomyces cerevisiae requires tyrosine and threonine phosphorylation of FUS3 and KSS1. Genes Dev. *6*, 1280–1292.

Gartner, A., Jovanovic, A., Jeoung, D.I., Bourlat, S., Cross, F.R., and Ammerer, G. (1998). Pheromone-dependent G1 cell cycle arrest requires Far1 phosphorylation, but may not involve inhibition of Cdc28-Cln2 kinase, in vivo. Mol. Cell. Biol. *18*, 3681–3691.

Harris, B.Z., Hillier, B.J., and Lim, W.A. (2001). Energetic determinants of internal motif recognition by PDZ domains. Biochemistry *40*, 5921–5930.

Heo, Y.S., Kim, S.K., Seo, C.I., Kim, Y.K., Sung, B.J., Lee, H.S., Lee, J.I., Park, S.Y., Kim, J.H., Hwang, K.Y., et al. (2004). Structural basis for the selective inhibition of JNK1 by the scaffolding protein JIP1 and SP600125. EMBO J. *23*, 2185–2195.

Hoffman, G.A., Garrison, T.R., and Dohlman, H.G. (2002). Analysis of RGS proteins in Saccharomyces cerevisiae. Methods Enzymol. *344*, 617–631.

Huse, M., and Kuriyan, J. (2002). The conformational plasticity of protein kinases. Cell *109*, 275–282.

Jacobs, D., Glossip, D., Xing, H., Muslin, A.J., and Kornfeld, K. (1999). Multiple docking sites on substrate proteins form a modular system that mediates recognition by ERK MAP kinase. Genes Dev. *13*, 163–175.

Jones, T.A., Zou, J.Y., Cowan, S.W., and Kjeldgaard (1991). Improved methods for binding protein models in electron density maps and the location of errors in these models. Acta Crystallogr. A *47*, 110–119.

Knighton, D.R., Zheng, J.H., Ten Eyck, L.F., Xuong, N.H., Taylor, S.S., and Sowadski, J.M. (1991). Structure of a peptide inhibitor bound to the catalytic subunit of cyclic adenosine monophosphate-dependent protein kinase. Science *253*, 414–420.

Kusari, A.B., Molina, D.M., Sabbagh, W., Jr., Lau, C.S., and Bardwell, L. (2004). A conserved protein interaction network involving the yeast MAP kinases Fus3 and Kss1. J. Cell Biol. *164*, 267–277.

Madhani, H.D., and Fink, G.R. (1997). Combinatorial control required for the specificity of yeast MAPK signaling. Science *275*, 1314–1317.

Madhani, H.D., and Fink, G.R. (1998). The riddle of MAP kinase signaling specificity. Trends Genet. *14*, 151–155.

Maleri, S., Ge, Q., Hackett, E.A., Wang, Y., Dohlman, H.G., and Errede, B. (2004). Persistent activation by constitutive Ste7 promotes Kss1-mediated invasive growth but fails to support Fus3-dependent mating in yeast. Mol. Cell. Biol. *24*, 9221–9238.

Navaza, J. (1994). AMoRe: an automated package for molecular replacement. Acta Crystallogr. A *50*, 157–163.

Otwinowski, Z., and Minor, W. (1997). Processing of x-ray diffraction data collected in oscillation mode. Methods Enzymol. *A276*, 307–325.

Perrakis, A., Harkiolaki, M., Wilson, K.S., and Lamzin, V.S. (2001). ARP/wARP and molecular replacement. Acta Crystallogr. D Biol. Crystallogr. *57*, 1445–1450.

Peter, M., Gartner, A., Horecka, J., Ammerer, G., and Herskowitz, I. (1993). FAR1 links the signal transduction pathway to the cell cycle machinery in yeast. Cell *73*, 747–760.

Sharrocks, A.D., Yang, S.H., and Galanis, A. (2000). Docking domains and substrate-specificity determination for MAP kinases. Trends Biochem. Sci. *25*, 448–453.

Sprague, G.F., Jr. (1991). Assay of yeast mating reaction. Methods Enzymol. *194*, 77–93.

Tanoue, T., and Nishida, E. (2003). Molecular recognitions in the MAP kinase cascades. Cell. Signal. *15*, 455–462.

Tanoue, T., Adachi, M., Moriguchi, T., and Nishida, E. (2000). A conserved docking motif in MAP kinases common to substrates, activators and regulators. Nat. Cell Biol. *2*, 110–116.

Vinciguerra, M., Vivacqua, A., Fasanella, G., Gallo, A., Cuozzo, C., Morano, A., Maggiolini, M., and Musti, A.M. (2004). Differential phosphorylation of c-Jun and JunD in response to the epidermal growth factor is determined by the structure of MAPK targeting sequences. J. Biol. Chem. *279*, 9634–9641.

Zarrinpar, A., Bhattacharyya, R.P., and Lim, W.A. (2003a). The structure and function of proline recognition domains. Sci. STKE *2003*, RE8.

Zarrinpar, A., Park, S.H., and Lim, W.A. (2003b). Optimization of specificity in a cellular protein interaction network by negative selection. Nature *426*, 676–680.

Zhan, X.L., Deschenes, R.J., and Guan, K.L. (1997). Differential regulation of FUS3 MAP kinase by tyrosine-specific phosphatases PTP2/PTP3 and dual-specificity phosphatase MSG5 in Saccharomyces cerevisiae. Genes Dev. *11*, 1690–1702.

Zhang, F., Strand, A., Robbins, D., Cobb, M.H., and Goldsmith, E.J. (1994). Atomic structure of the MAP kinase ERK2 at 2.3 A resolution. Nature *367*, 704–711.

Accession Numbers

The coordinates of Fus3 and the Fus3/Ste7_pep1, Fus3/Msg5_pep, and Fus3/Far1_pep complexes are deposited in the Protein Data Bank with the ID codes 2B9F, 2B9H, 2B9I, and 2B9J, respectively.